Langmuir

Article

pubs.acs.org/Langmuir

Water-Stable Three-Dimensional Ultrafine Fibrous Scaffolds from Keratin for Cartilage Tissue Engineering

Helan Xu,[†] Shaobo Cai,[†,‡] Lan Xu,[§] and Yiqi Yang*[,†,‡,∥,⊥]

[†]Department of Textiles, Merchandising and Fashion Design, 234, HECO Building, University of Nebraska—Lincoln, Lincoln, Nebraska 68583-0802, United States

[‡]Key Laboratory of Science and Technology of Eco-Textiles, Ministry of Education, Donghua University, Shanghai 201620, China

[§]Department of Agronomy and Horticulture, University of Nebraska—Lincoln, 279 Plant Science Hall, Lincoln, Nebraska 68583-0915, United States

[∥]Department of Biological Systems Engineering and [⊥]Nebraska Center for Materials and Nanoscience, 234 HECO Building, University of Nebraska—Lincoln, Lincoln, Nebraska 68583-0802, United States

ABSTRACT: Intrinsically water-stable scaffolds composed of ultrafine keratin fibers oriented randomly and evenly in three dimensions were electrospun for cartilage tissue engineering. Keratin has been recognized as a biomaterial that could substantially support the growth and development of multiple cell lines. Besides, three-dimensional (3D) ultrafine fibrous structures were preferred in tissue engineering due to their structural similarity to native extracellular matrices in soft tissues. Recently, we have developed a nontraditional approach to developing 3D fibrous scaffolds from alcohol-soluble corn protein, zein, and verified their structural advantages in tissue engineering. However, keratin with highly cross-linked molecular structures could not be readily dissolved in common solvents for fiber spinning, which required the remarkable drawability of solution. So far, 3D fibrous scaffolds from pure keratin for biomedical applications have not been reported. In this research, the highly cross-linked keratin from chicken feathers was de-cross-linked and disentangled into linear and aligned molecules with preserved molecular weights, forming highly stretchable spinning dope. The solution was readily electrospun into scaffolds with ultrafine keratin fibers oriented randomly in three dimensions. Due to the highly cross-linked molecular structures, keratin scaffolds showed intrinsic water stability. Adipose-derived mesenchymal stem cells could penetrate much deeper, proliferate, and chondrogenically differentiate remarkably better on the 3D keratin scaffolds than on 2D PLA fibrous scaffolds, 3D soy protein fibrous scaffolds, or 3D commercial nonfibrous scaffolds. In summary, the electrospun 3D ultrafine fibrous scaffolds from keratin could be promising candidates for cartilage tissue engineering.

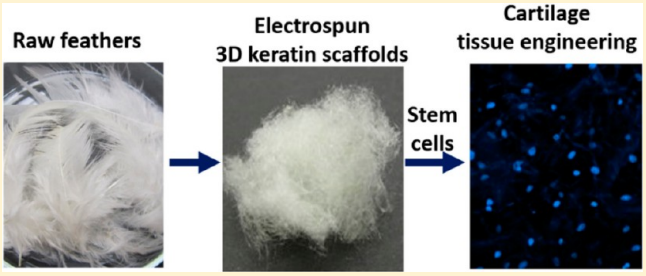

INTRODUCTION

In tissue engineering, three-dimensional (3D) ultrafine fibrous structures are preferred due to their structural similarity to native extracellular matrices (ECMs).[1] Ultrafine here refers to a diameter smaller than 10 μm.[2,3] However, technical difficulty remained in fabricating scaffolds composed of 3D-oriented nano- or microfibers from proteins.[4] Phase separation and electrospinning were the major methods used to develop 3D fibrous structures. Phase separation was limited to certain water-soluble proteins, such as gelatin,[5] while electrospinning had much broader applicability and was used to develop various protein scaffolds, including collagen,[6] silk fibroin,[7,8] and zein.[9,10] However, electrospinning usually generated fibrous mats with fibers oriented in two dimensions (2D). These 2D fibrous mats had compact structures with no fibers oriented outside the horizontal directions and thus notably restricted cell penetration and orientation in the directions intersecting with the horizontal plane. Therefore, applications of 2D fibrous scaffolds in repairing tissues or organs with certain thickness and cell penetration were limited. To improve the cellular accessibility and bulkiness of electrospun scaffolds, a conventional electrospinning method has been modified by incorporating coarse fibrous frames[11] or porogens[12] and using a coagulation bath instead of conventional solid boards to collect fibers.[13] However, the resultant less-tight structures retained the 2D arrangement of the nanofibers, with little fiber oriented in the vertical and any inclined planes.

Keratin, the protein largely present in poultry feathers and hairs and horns of animals with natural water stability, has been proven to be a promising substrate for biomedical applications. As a protein, keratin has molecular structures similar to those of collagen, the prominent protein in native ECMs. Furthermore, keratin had tripeptides Arg-Gly-Asp (RGD) and Leu-Asp-Val (LDV) that could bind with cell surface ligands and thus could promote cell adhesion.[14] In addition, due to the high cross-linking degree, keratin might not have poor water stability,

Received: February 25, 2014
Revised: June 18, 2014
Published: July 10, 2014

   dx.doi.org/10.1021/la500768b | Langmuir 2014, 30, 8461−8470

the prominent problem that restricted the medical applications of many proteins.

To the best of our knowledge, keratin has not been developed into 100% ultrafine fibers for medical applications. So far, keratin in the forms of films, sponges, and hydrogels showed satisfactory support for multiple cell lines. Recently, Reichl produced keratin films to culture corneal epithelial cells,[15] and Tachibana produced keratin sponges for the in vitro culture of osteoblasts and fibroblasts,[16,17] and Burnett developed keratin hydrogels as hemostats.[14] It could be inferred that fibrous forms may even enhance the biological performance of keratin biomaterials. However, the reported fibrous keratin materials were usually fabricated after blending with other natural polymers, including chitosan[18] and silk fibroin,[19] or synthetic polymers, including poly(lactic acid)[20] and poly(ethylene glycol).[21] Poor solubility of keratin in common solvents may be an obstacle for the development of fibers, especially ultrafine fibers. To fabricate 3D ultrafine fibrous scaffolds, keratin solution in certain solvents should have good drawability, which could be directly related to the viscosity of protein solutions.[22] Acceptable viscosity for fiber spinning required macromolecules to align in the solution with a certain degree of entanglement. Surfactants have been long studied for their ability to increase the viscosity of a macromolecule solution, including proteins, via forming complexes with macromolecules. The mechanism was the alkyl tails of surfactant being bound with polypeptides via hydrophobic interaction and thus the hydrophilic heads being left on the surface to contact water molecules. The introduced strong molecular electrical repulsion forced the molecules to align and disentangle. For example, sodium dodecyl sulfate (SDS), a widely used anionic surfactant, has been reported to increase the viscosity of PEG,[23] lysozyme,[24] and trypsin.[25] However, surfactant−macromolecule interaction was intensively investigated using only water-soluble macromolecules instead of water-insoluble molecules. Recently, we employed the mechanism and successfully electrospun zein, the corn protein dissolved with SDS, to develop 3D fibrous scaffolds.[26] Zein had a negligible number of disulfide cross-links and was very soluble in common solvents.[27,28] However, so far, no effective method has been employed to dissolve highly cross-linked proteins, such as keratin, for fiber spinning.

Cartilage lacks the self-healing capacity and thus necessitates tissue engineering scaffolds for their regeneration.[29] Since cartilage has a major portion of ECMs typically composed of ultrafine fibers oriented in three dimensions, 3D ultrafine fibrous scaffolds are preferred in cartilage tissue engineering. Meanwhile, mesenchymal stem cells (MSCs) were promising cell sources for cartilage tissue engineering. Among various types of MSCs, adipose-derived mesenchymal stem cells (ADMSCs) with much larger availability and the potential for chondrogenic differentiation could be used for cartilage tissue engineering.[30] The proper development of the differentiation of stem cells into chondrocytes requires 3D fibrous environments.[31]

Though collagen was the major protein in natural cartilage, we believe keratin is a better material for cartilage tissue engineering due to its similar biocompatibility but much better water stability. First, similar to collagen, keratin also has RGD and LDV motifs in the molecules to bind cells. Moreover, in cartilage tissue engineering, long-term water stability was an indispensable quality for materials, and thus the more water-stable keratin was preferred to collagen. In an in vitro study targeting cartilage tissue regeneration, scaffolds should provide long-term support to cells, especially to stem cells. Furthermore, in in vivo cartilage repair, the cartilage tissue without blood vessels could only grow and repair slowly and thus also needed the scaffolds to be stable for a long time to support the growth of chondrocytes or other seeding cells. However, tissue engineering scaffolds from collagen showed poor to fair water stability even after cross-linking,[6] which possibly brought about problems of toxicity.

In this paper, keratin extracted from feathers was dissolved in aqueous solution with SDS and then electrospun into scaffolds composed of 3D randomly oriented ultrafine fibers for the first time. The scaffolds showed satisfactory water stability. ADMSCs were cultured on the 3D ultrafine fibrous keratin scaffolds and induced to differentiate into chondrocytes. On the basis of biochemical assays, the 3D keratin scaffolds showed better support for the proliferation and differentiation of ADMSCs than did 2D fibrous PLA scaffolds, 3D commercial nonfibrous scaffolds, and 3D ultrafine soy protein scaffolds.

EXPERIMENTAL SECTION

Materials. Chicken feather barbs were provided by Featherfiber Corporation (Nixa, MO). Sodium dodecyl sulfate (SDS, 99.0%) was purchased from Hoefer Inc. (San Francisco, CA), and urea (99.0%) was supplied by Oakwood Chemical Inc. (West Columbia, SC). Sodium carbonate, sodium bicarbonate, sodium sulfate, acetone, potassium chloride, and sodium hydroxide were purchased from BDH Chemicals Inc. (West Chester, PA). Cysteine was supplied by Amresco LLC. (Solon, OH). Poly(lactic acid) (PLA) was provided by Cargill Dow LLC Films (Minneapolis, MN). Soy protein (PRO-FAM 646) was supplied by ADM International (Decatur, IL).

Major chemicals used in this process were either derived from renewable resources or could be reused. As an environmentally benign reducing agent, cysteine can be commercially produced via fermentation.[32] SDS could be synthesized by treating lauryl alcohol with sulfur trioxide gas, while the lauryl alcohol was usually derived from the hydrolysis of vegetable oils, such as coconut oil or palm oil.[33]

Controlled Cleavage of Disulfide Cross-Links in Feathers. Keratin from feathers was extracted under mild alkaline conditions to break the disulfide cross-links and preserve the backbones. The weight ratio of 8 M urea solution to chicken feathers of 17:1 was used to immerse the chicken feathers completely, and the treatment temperature was 70 °C. About 10% of cysteine based on the weight of chicken feathers was added to the solution. The pH was adjusted to around 10.5 using a 50% NaOH solution, and the treatment time was 12 h.[34]

After treatment, the solution was centrifuged at 8000 rcf for 20 min to precipitate undissolved feather residues. The supernatant was adjusted to pH 4 using hydrochloric acid and sodium sulfate to precipitate dissolved keratin. The keratin precipitate was washed three times with distilled water under centrifugation of 8000 rcf for 20 min. The collected keratin was dried at 50 °C and pulverized. Soy protein was extracted using the same procedures. Keratin treated using 5% NaOH according to the literature was used as a comparison.[35]

Molecular Weight Measurement. Sodium dodecyl sulfate-polyacrylamide gel electrophoresis (SDS-PAGE) was used to evaluate the molecular weight of keratin samples, including raw feathers, feathers treated using 5% NaOH in the electrospinning of PVA/keratin, and keratin obtained in this research. About 1 mg of each sample was dissolved in 100 μL NuPAGE LDS sample buffer (1×), held at 70 °C for 10 min, and left standing at room temperature for 2 h. The solution was vortex mixed prior to loading. For each slot of the gel, each 10 μL sample was loaded. After electrophoresis, the gel was fixed with 10% acetic acid and isopropyl ethanol, stained with Coomassie brilliant blue G-250 for 2 h at room temperature, and then destained in 10% acetic acid until a clear background could be observed. The molecular weights of the protein standard mixture range from 4 to 250 kDa.

Electrospinning of Three-Dimensional Fibrous Keratin Scaffolds, Three-Dimensional Fibrous Soy Protein Scaffolds, and Two-Dimensional Fibrous PLA Scaffolds. To fabricate 3D ultrafine fibrous keratin scaffolds, we dissolved extracted keratin in

dx.doi.org/10.1021/la500768b | Langmuir 2014, 30, 8461−8470

0.3 M sodium carbonate−bicarbonate buffer in a weight ratio of 25%. SDS with the same weight of keratin was added to the dispersion for dissolution. The mixture was heated under stirring at 90 °C for 1 h. The solution was loaded into a syringe and electrospun under a voltage of 45 kV. The distance between the collection board and syringe needle was 25 cm. The needle of the syringe was negatively charged, and the collection board was positively charged. Soy protein as is has been electrospun into 3D ultrafine fibrous scaffolds after being dissolved with SDS.[36,37]

For comparison, PLA was electrospun into a 2D fibrous mat. PLA was dissolved in chloroform in a weight ratio of 7% and aged for 24 h. Electrospun PLA fiber mats were produced by extruding the PLA solution at a rate of 1 mL h^{-1} with an applied voltage of 18 kV. The distance between the needle and surface of the winding drum was kept at 15 cm, and the rotational rate of the drum was 1200 rpm.

Morphologies of Three-Dimensional Fibrous Keratin Scaffolds. Photographs of 3D fibrous keratin scaffold were taken using a digital camera. Morphologies of the 3D fibrous keratin scaffolds were observed under a Hitachi S-3000N scanning electron microscope (SEM), and the interior structure of the 3D keratin scaffolds after the removal of SDS was observed in the wet state using a confocal laser scanning microscope (CLSM) in both the longitudinal and transverse directions. Fiber diameters were obtained by measuring 30 fibers in SEM images.

To evaluate the porosity of the 3D scaffolds from keratin and soy protein, a specific pore volume of scaffolds as shown in eq 1 was selected. The scaffolds were frozen in liquid nitrogen and then cut into regular shapes using a sharp blade. The length, width, and thickness of the scaffolds were measured, as was the mass of the scaffolds.

$$V_{sp} = \frac{V_{pore}}{m_{scaffold}} = \frac{V_{scaffold}}{m_{scaffold}} - \frac{1}{\rho_{material}} \quad (1)$$

where V_{sp} is the specific pore volume, V_{pore} is the volume of pores in the scaffolds, $m_{scaffold}$ is the mass of the scaffolds, $V_{scaffold}$ is the volume of the scaffolds calculated on the basis of the precisely measured length, width, and thickness of scaffolds, and $\rho_{material}$ is the density of the material.

Fourier Transform Infrared (FTIR) Spectroscopy. FTIR spectra of the raw chicken feathers and electrospun 3D ultrafine fibrous keratin scaffolds were collected on an attenuated-reflectance ATR spectrophotometer (Nicolet 380, Thermo-Fisher, Waltham, MA) to determine the secondary structures of the keratin samples. The samples were placed on a diamond plate, and 64 scans were collected for each sample at a resolution of 64 cm^{-1}.

Water Stability. Keratin scaffolds were tested for water stability in PBS solutions with a liquor ratio of 20:1 at 37 °C. At various time points, 0, 5, 10, 15, 25, and 35 days, scaffolds were taken out of the solution, rinsed with distilled water, and freeze dried. The change in the morphologies of keratin scaffolds was observed under SEM.

Compression Analysis. The wet and dry compression properties of 3D electrospun keratin scaffolds were tested on a TA.XT.Plus texture analyzer (Texture Technologies Corp., Scarsdale, NY). The electrospun 3D keratin scaffolds without SDS in the dry state, immersed in PBS for 3 days at 37 °C and in PBS for 6 days at 37 °C, were tested. All of the samples had a thickness of between 20 and 30 mm. The unconfined compression property was measured using a 0.5-in.-diameter flat plastic plunger at a speed of 1 mm/s until 40% strain was reached.

Cultivation of Adipose-Derived Mesenchymal Stem Cells. To evaluate the potential of 3D electrospun keratin ultrafine fibrous structures as scaffolds for cartilage tissue engineering, adipose-derived mesenchymal stem cells (ADMSCs, ATCC PCS-500-011, Manassas, VA) were cultured on electrospun 3D keratin scaffolds, 2D PLA scaffolds, and commercial 3D scaffolds (Biomerix 3D Scaffold, Fremont, CA). Commercial 3D scaffolds were open-cell macroporous structures of polycarbonate polyurethane−urea (PCPU) with a void content higher than 90%.

Cell Seeding. The electrospun 3D keratin scaffolds were rinsed in 60% acetone solution with 10% potassium chloride for 5 days and distilled water for 2 days and then freeze dried.[38] The high solubility of SDS in acetone solution with KCl resulted in the thorough removal of SDS. For cell seeding, specimens weighing 10 mg from each scaffold sample were prepared. The scaffolds were sterilized under 120 °C for 1 h in an autoclave. The commercial 3D scaffolds were immersed in 70% aqueous ethanol overnight for sterilization. After sterilization, all of the scaffolds were rinsed in PBS before cell culturing. All scaffolds were placed in 48-well culture plates (TPP Techno Plastic Products, Switzerland). ADMSCs were seeded onto the scaffolds with a density of 3×10^5 cells mL^{-1} along with 500 μL of Dulbecco's modified eagle's medium (DMEM, with 10% FBS, 1% antibiotic solution) at 37 °C in a humidified 5% CO_2 atmosphere.

Cell Attachment and Proliferation. MTS assays were performed to quantitatively investigate cell viability at attachment and proliferation stages. At each time point, 4 h, 5 days, 10 days, and 15 days, the samples were washed with PBS, placed in new 48-well plates containing 450 μL $well^{-1}$ 20% MTS reagent (CellTiter 96 Aqueous One Solution Cell Proliferation Assay, Promenade) in DMEM, and incubated at 37 °C in a humidified 5% CO_2 atmosphere for 3 h. After incubation, 150 μL of the solution from each well was pipetted into a 96-well plate, and the optical densities were measured at 490 nm using a UV/vis multiplate spectrophotometer (Multiskan Spectrum, Thermo Scientific, Waltham, MA). The MTS solution in DMEM without cells served as the blank. For each data point, at least four samples were tested.

Chondrogenic Differentiation of ADMSCs. ADMSCs were seeded onto all scaffolds placed in 48-well culture plates at a density of 3×10^5 cells mL^{-1} and 500 μL $well^{-1}$ in DMEM (with 10% FBS, 1% antibiotic solution) at 37 °C in a humidified 5% CO_2 atmosphere and were allowed to adhere for 24 h. After 24 h, DMEM was replaced with a chondrogenic differentiation medium (chondrocyte differentiation tool kit, ATCC PCS-500-051, Manassas, VA). The chondrogenic differentiation medium was renewed every 3 or 4 days.

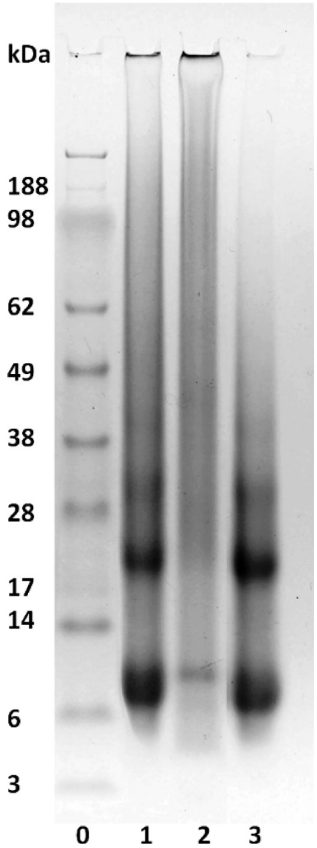

Figure 1. SDS-PAGE of 0, standard protein markers; 1, raw chicken feathers; 2, NaOH extracted keratin; and 3, keratin extracted in the research.

dx.doi.org/10.1021/la500768b | Langmuir 2014, 30, 8461−8470

Scheme 1. Three-Dimensional Deposition of Keratin Fibers during the Electrospinning Processes[a]

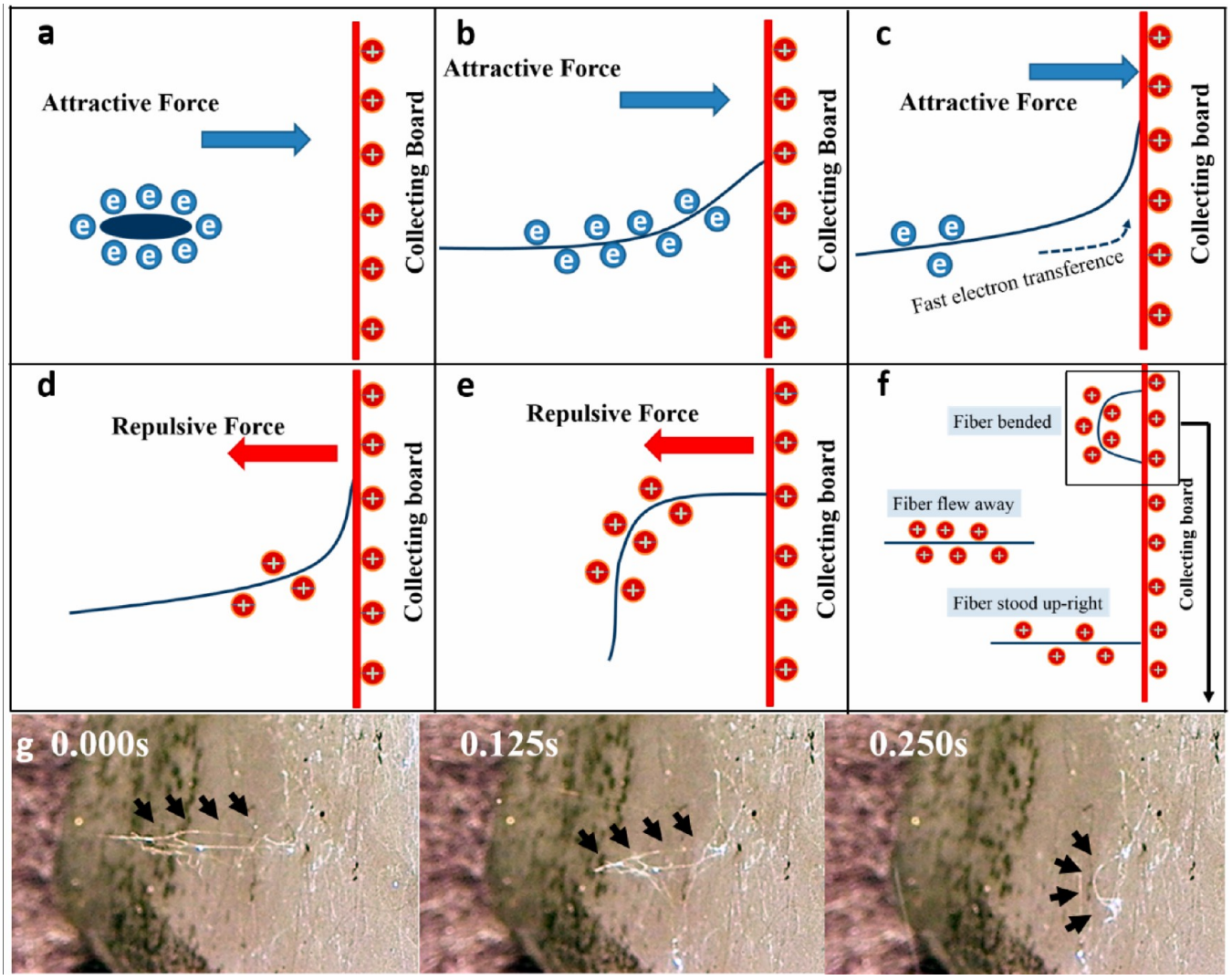

[a]The spinning dope was negatively charged, and the collecting board was positively charged. Red bar, collecting board; red circle, positive charge; blue ellipse, keratin solution drop; blue curve, keratin fibers; blue arrow, attractive force; dashed blue arrow, direction of electron transference; red arrow, repulsive force; blue circle with "e", electron. A series of digital photographs of the deposition of arched fibers taken with a time interval of 0.125 s are shown at the bottom of panel g. The black arrows indicated the position of the fiber bundle.

Biochemical Assays. Glycosaminoglycan (GAG) and collagen were the specific macromolecules that can be secreted specifically after the chondrogenic differentiation was initiated for ADMSCs. The scaffolds cultured with ADMSCs for 5, 10, and 15 days were washed three times in PBS before measurements of GAGs and collagen. The content of GAGs was determined using a GAG assay kit (Astarte Biologics, Redmond, WA) following the protocol in the assay kit. The optical density was measured using a UV/vis multiplate spectrophotometer at 525 nm. The number of GAGs was divided by the initial weights of the samples to determine the ability of the samples to support the chondrogenic differentiation of different scaffolds. Total collagen was measured using a Sirius red total collagen detection kit (Chondrex, Inc., Redmond, WA) following the standard protocols provided with the assay kit. The newly secreted total collagen in the scaffold−cell complex was determined by digesting first the scaffold−cell complex with papain solution and then dyed collagen with Sirius red. Sirius red is a unique dye which specifically binds to the $[Gly\text{-}X\text{-}Y]_n$ helical structure in collagen. A calibration curve was obtained by using the collagen standard in the assay kit. Every six scaffolds under each condition were used for measurement in order to calculate the means and standard deviations.

Statistical Analysis. All of the data obtained were analyzed by one-way analysis of variance with the Scheffé test with a confidence interval of 95%. A p value smaller than 0.05 indicated a statistically significant difference. Standard deviations were shown by the error bars in figures, and the data in the figures labeled with different numbers or characters indicated significant differences among each other.

RESULTS AND DISCUSSION

Extraction of Keratin. Figure 1 demonstrates the distribution of molecular weights of untreated chicken feathers in lane 1, NaOH extracted feather keratin in lane 2, and keratin extracted under conditions developed in this research in lane 3. The soluble portion of untreated chicken feathers showed strong bands at around 10 and 20 kDa, a weak band at around 30 kDa, and a smear between 20 and 188 kDa. Similarly, the keratin extracted under reductive and mild alkaline condition also had strong bands at 10 and 20 kDa, a weak band at around 30 kDa, and a weak smear existing between 30 and 62 kDa. It could be inferred that the reductive and mild alkaline condition

dx.doi.org/10.1021/la500768b | Langmuir 2014, 30, 8461−8470

could preserve the backbones of keratin molecules much better than the strong alkaline condition. The molecular weight of the extracted keratin was suitable for fiber spinning, as indicated previously.[39] On the contrary, the NaOH dissolved feather keratin showed a smear only from the top to 20 kDa with a lighter shade and a weak band at around 10 kDa. This was due to the random breaking of backbones of feather keratin. The alkaline-treated keratin was usually blended with synthetic polymers for electrospinning since the viscosity of the keratin with randomly distributed molecular weights might not be adequate for spinning.[20]

During extraction, the synergistic effects of swelling and reduction under mild alkaline conditions led to a high yield (>70%) of keratin with effectively preserved backbones. In the 8 M urea solution, urea disrupted inter- and intramolecular hydrogen bonds and weakened the hydrophobic interaction between polypeptides after being concentrated on the surface of protein. This led to the exposure of polypeptides in the solvent and thus facilitated the reaction of cysteine with disulfide bonds that used to be buried inside the peptide assembly. As a result, the disulfide bonds could be efficiently cleaved while the backbones were not remarkably affected.

Mechanism of Three-Dimensional Electrospinning. Scheme 1 briefly demonstrates the process of 3D deposition of ultrafine keratin fibers during electrospinning. The key step of dissolution, the addition of SDS, induced a change in the surface conductivity and subsequently resulted in the 3D deposition of fibers.[26] During dissolution, alkyl C12 tails of SDS and hydrophobic domains of keratin were integrated via hydrophobic interaction, while the sulfate groups of SDS remained on the surface of the SDS−keratin complex. The strong negative charge of the complexes induced strong repulsions among each other and resulted in the disentanglement of protein molecules and successful dissolution. Verification of the mechanism of 3D electrospinning using corn protein was discussed in detail in our previous research.[26]

During electrospinning, the keratin−SDS solution was negatively charged, and thus the surface of the spinning dope showed a strong negative charge.[26] As shown in Scheme 1a, the solution droplet of the protein/SDS complex flew to the positively charged collecting board. During the flying process, the drop was stretched into a fiber with a larger length to diameter ratio and hit the board with one fiber end, as shown in Scheme 1b. Scheme 1c demonstrates that the electrons on the fibers tranferred to the collecting board in a fast manner due to the high surface conductivity, attributed to the negative sulfate groups of SDS on the keratin/SDS complex. Transiently, the fiber carried positive charge before completely attaching to the board as shown in Scheme 1d. The attraction force between the fiber and the board became repulsive, and thus the fiber was rejected by the board as shown in Scheme 1e. Scheme 1f illustrates three different states of keratin fibers after being driven back by the electrical repulsion. If the fibers were shorter and tranferred their electrons before the rear ends could attach to the board, then they could either stand upright on the board or fly away from the board. In another case, if the fibers were relatively long, then the negatively charged rear end of the fiber might be attracted to the collecting board before being transferred to the board, while the middle portion of the fiber carrying positive charge was repelled by the board. As a result, the fiber formed an arch on the collecting board. The deposition of arched/bent fibers is illustrated in the photographs in Scheme 1g. The front and rear ends of the fiber bundle attached to the collection board while the middle portion of the bundle was suspended above the board. Since the orientation varied throughout the middle segment of the arched fiber, continuous random deposition of the arched/bended fibers and fiber bundles contributed to the random arrangement of fibers within the whole 3D keratin scaffolds.

Morphology. Figure 2 demonstrates the front and side views of a typical 3D keratin fibrous scaffold using different

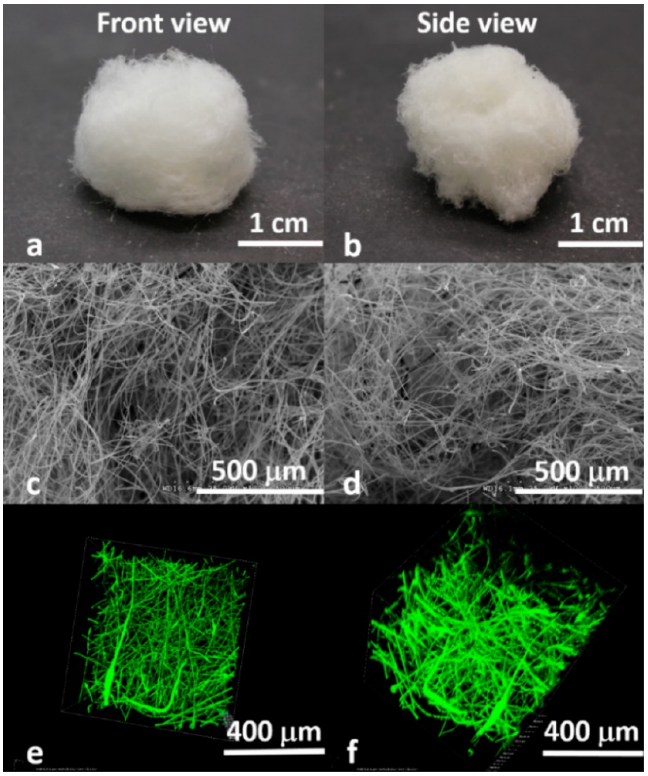

Figure 2. Morphologies of 3D electrospun keratin ultrafine fibrous scaffold. (a) Digital photograph of the front view, (b) digital photograph of the side view, (c) SEM image of the front view at a magnification of 100×, (d) SEM image of the side view at a magnification of 100×, (e) CLSM image of the front view in the wet state (100×), and (f) CLSM image of the view from 45° in the wet state (100×).

techniques at different magnifications. All of the images verified that the fibers were oriented randomly in horizontal and other directions in either the dry or wet state. As the front and side views of 3D keratin scaffolds in Figure 2a,b show, the scaffold can be a fluffy sphere with a diameter as large as 2 cm. The interior structures of the fibrous sphere in the dry state could be found to be oriented randomly in different directions spacially, as illustrated in Figure 2c,d. Besides, the inner structures of 3D electrospun keratin scaffolds in the wet state after the removal of SDS in Figure 2e,f proved that the fibers maintained their morphologies and arrangements in the wet state. Specifically, the CLSM image from the 45° view in Figure 2f illustrates that the wet keratin scaffolds have fibers oriented and distributed randomly in all three planes in the scaffolds. The 3D soy protein scaffolds showed similar morphologies to the 3D keratin scaffolds. The results were not demonstrated in this research.

There were continuous fibers in the 3D electrospun scaffolds. Many fibers aligned vertically in Figure 2c,d because we broke

dx.doi.org/10.1021/la500768b | Langmuir 2014, 30, 8461−8470

the whole piece of scaffolds to show the interior of the scaffolds instead of the surface. The 3D electrospinning could generate fluffy scaffolds with fibers randomly oriented in three dimensions (Figure 2f), especially in the inclined planes. However, the conventional 2D electrospinning could lead only to compact structures with fibers oriented in planar directions but not in the thickness directions.[26] Overall, scaffolds from 3D electrospinning could better guide cells to grow and spread spatially and penetrate more deeply into the interior of scaffolds to generate more-uniform new tissues.

The 3D keratin scaffolds had diameters of around 4.8 ± 4.0 μm, while the 3D soy protein scaffolds had diameters of around 4.5 ± 3.8 μm. The specific pore volume of 3D keratin scaffolds was 193.1 ± 12.6 cm^3/g, while that of 3D soy protein scaffolds was 185.6 ± 17.5 cm^3/g.

Protein Conformation. Figure 3 shows the FTIR spectra of untreated chicken feathers and 3D electrospun keratin

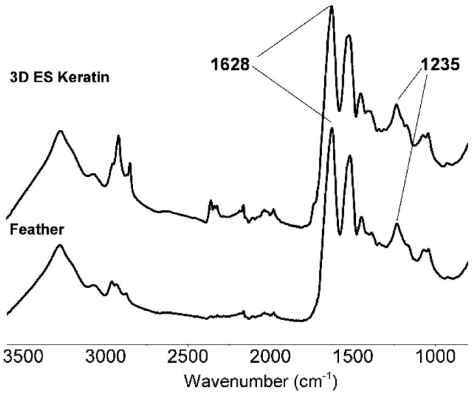

Figure 3. FTIR spectra of raw chicken feathers and 3D electrospun keratin ultrafine fibrous scaffolds after the removal of SDS.

ultrafine fibrous scaffolds after the removal of SDS from 800 to 3500 cm^{-1}. In the spectra, the characteristic bands for proteins could be observed, including N−H stretching at around 3300 cm^{-1} and C−H stretching at 3070 cm^{-1}, C−O stretching from 1600 to 1700 cm^{-1} for amide I, N−H deformation from 1500 to 1550 cm^{-1} for amide II, and N−H deformation from 1200 to 1300 cm^{-1} for amide III.[40] The peaks at 1628 and 1235 cm^{-1} in the amide I and III bands represent the β-sheet conformation of protein. In terms of secondary structure, the electrospun keratin scaffolds with evident β-sheet conformation showed a strong similarity to untreated chicken feathers. It could be inferred that the driving force during electrospinning could effectively induce the formation of the β-sheet and that SDS could be efficiently removed after washing. The regeneration of the β-sheet conformation in electrospun ultrafine keratin fibers could lead to good water stability of the scaffolds, while the removal of SDS was the premise of in vitro cell culture.

Water Stability. In Figure 4, it can be observed that the 3D electrospun ultrafine keratin fibers could preserve their fibrous morphologies even after immersion in PBS at 37 °C for as long as 35 days. There was a slight increase in the diameters of fibers after being incubated for 25 and 35 days. Remarkably, the porous structures of the scaffolds were not jeopardized with this extent of fiber swelling. It could be predicted that the keratin ultrafine fibers should be able to retain their fibrous structures for an even longer time under wet conditions.

It has been widely recognized that the poor water stability of protein-based biomaterials critically restricted their biomedical applications. However, most of the cross-linked protein scaffolds showed either impaired biocompatibility or limited improvement in water stability. Here, the pure keratin scaffolds without any external cross-linking had remarkably better water stability than most widely used protein biomaterials, including collagen, gelatin, albumin, and zein. For example, the zein scaffolds cross-linked with citric acid could not retain their fibrous morphologies after incubation in PBS for 15 days,[8] and the EDC-NHS cross-linked collagen fibers could merely retain their morphology after being placed in 55% relative humidity for 1 day.[41] The intrinsic water stability made ultrafine keratin fibers desirable for biomedical applications.

Culture of ADMSCs. Proteins with sufficient water stability could be ideal materials for long-term cell culture, such as stem cell culture. So far, most of the work regarding stem cell differentiations has been carried out on 3D scaffolds composed of synthetic fibers because synthetic polymers could be easily fabricated into fibers and did not degrade very fast. But synthetic polymers were not optimal cell culture substrates because they were usually hydrophobic and were not preferred for cell attachment. On the contrary, natural polymers, including proteins, facilitated cell attachment and proliferation, but their short-term degradation and dimensional instability in aqueous environments prevented their wide biomedical application. The water stability and good biocompatibility of keratin substrates made 3D keratin substrates promising for

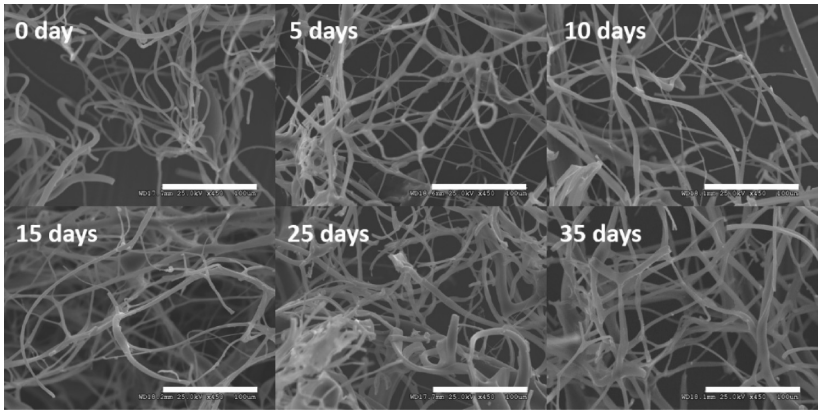

Figure 4. Water stability of 3D electrospun ultrafine keratin fibers after immersion in PBS at 37 °C for 0, 5, 10, 15, 25, and 35 days. The scale bar represents 100 μm.

dx.doi.org/10.1021/la500768b | Langmuir 2014, 30, 8461−8470

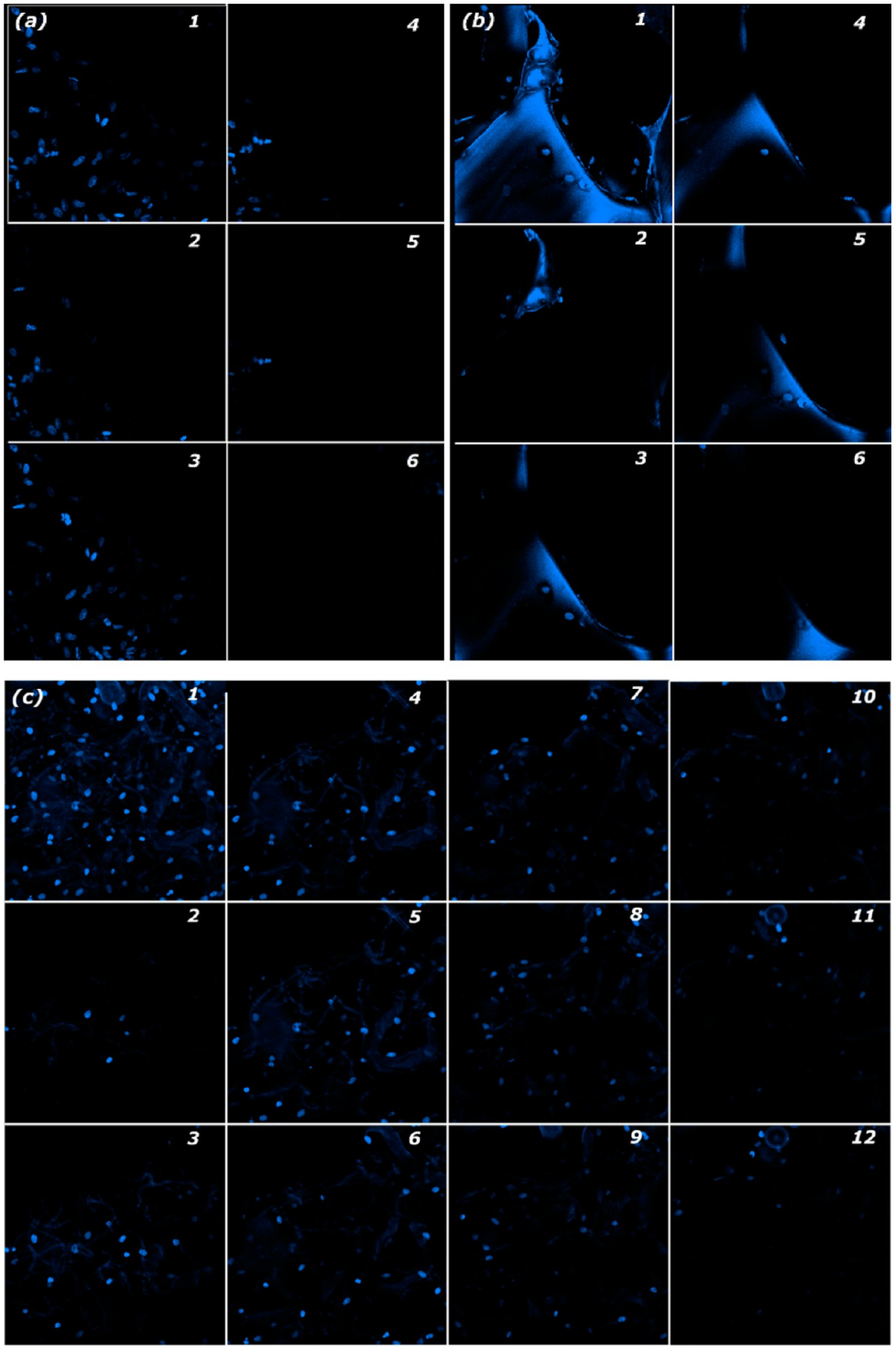

Figure 5. Penetration of ADMSCs in (a) 2D PLA fibrous scaffolds, (b) 3D commercial scaffolds, and (c) 3D keratin fibrous scaffolds 5 days after seeding. The CLSM montage images were taken in sequential sections at 15 μm intervals at 60×. The blue dots represent nuclei of cells stained with Hoechst 33342. The first picture with a label of "1" in each panel is a combination of all of the other pictures in the panel.

stem cell culture. The cell culture results also proved that SDS had been thoroughly eliminated from the scaffolds.

Cell Penetration. Figure 5 demonstrates that ADMSCs in electrospun 3D ultrafine fibrous keratin scaffolds could penetrate more deeply and distribute more uniformly compared to those in 2D PLA fibrous scaffolds or in 3D commercial scaffolds. In Figure 5c, the cells could be found 165 μm under the surface and were distributed uniformly on each plane of the 3D ultrafine fibrous keratin scaffold. The keratin fibers were distributed evenly in the 3D fibrous structures, leading to the formation of uniform porous structures. As a result, the cells attached to the keratin fibers were evenly spaced in the structures. It could be inferred that, with a longer culturing time, the cells may penetrate more deeply into the structures. In Figure 5a, cells could not be observed 60 μm below the surface of the PLA 2D scaffold, and the distribution of cells was

dx.doi.org/10.1021/la500768b | *Langmuir* 2014, 30, 8461−8470

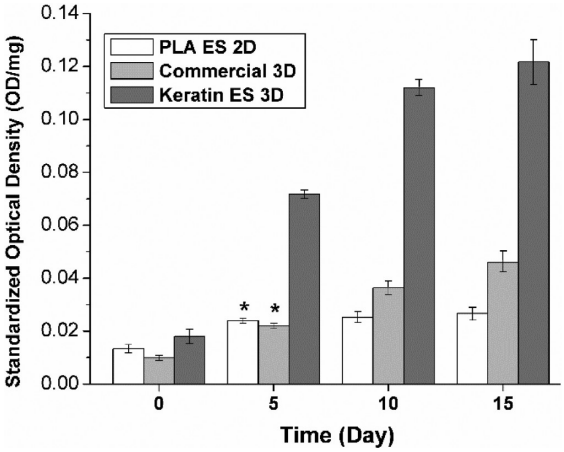

Figure 6. Attachment and proliferation of ADMSCs on 2D electrospun PLA scaffolds, 3D commercial scaffolds, and 3D electrospun keratin scaffolds. Data labeled with the same symbols were not significantly different from each other.

Table 1. Comparison among Ratios of Cell Attachment and Proliferation on 3D Keratin Fibrous Scaffolds/2D PLA Fibrous Scaffolds with 3D Keratin Fibrous Scaffolds/3D Commercial Scaffolds and 3D Soy Protein Fibrous Scaffolds/3D Commercial Scaffolds

ratio of MTS reading of cells on 3D scaffolds to that on controls	4 h	5 days	10 days	15 days
3D keratin/2D PLA	1.4	3.0	4.4	4.6
3D keratin/3D commercial	1.8	3.3	3.1	2.6
3D soy protein/3D commercial	2.1	2.9	2.7	2.2

not even. This difference indicated that the tight packing of fibers in the 2D scaffolds led to low interconnectivity in between the structures and subsequently restricted the penetration of cells. As shown in Figure 5b, cells could be observed 75 μm under the surface of the commercial 3D porous scaffold. However, it could be noticed that the distribution of cells was very uneven, since the cells could attach only to the walls of the scaffold. The uneven distribution of cells in the commercial 3D porous scaffold may cause the formation of uneven cartilage tissue in long-term cell culture. As a consequence, 3D ultrafine fibrous keratin scaffolds could facilitate even migration and penetration of cells into the interior of the structures and showed the capability to support the formation of cartilage tissue of a certain depth in long-term in vivo cartilage reparation processes.

Attachment and Proliferation of ADMSCs. Figure 6 depicts the attachment and proliferation of ADMSCs on 2D electrospun PLA scaffolds, 3D commercial PCPU porous scaffolds, and 3D electrospun fibrous keratin scaffolds using the MTS assay. Four hours after cell seeding, the attachment of ADMSCs on 3D keratin scaffolds was 1.4 and 1.8 times that on 2D PLA and 3D commercial scaffolds, as summarized in Table 1. Moreover, cells seeded on 3D keratin scaffolds grew and proliferated in a much faster manner than those on 2D PLA scaffolds. Therefore, the ratios of cell activity on 3D scaffolds to that on 2D PLA scaffolds kept on increasing. This could be because the tight packing of nanoscale PLA fibers limited the infiltration of cells into the 2D PLA scaffolds as shown in Figure 6a, while there was not accessible space in 3D scaffolds. As a resultant, the number of cells on 2D PLA scaffolds did not increase remarkably after 10 days of culturing, while the cells on the other 3D scaffolds still proliferated significantly. On the other hand, the cells on 3D keratin scaffolds proliferated faster than those on 3D commercial scaffolds, as shown in Table 1. Furthermore, cell culture results on the 3D keratin scaffolds were compared to that on 3D soy protein scaffolds with similar morphological properties. The ratios of MTS reading indicating cell activity on 3D keratin to 3D soy protein scaffolds were similar at the attachment stage but significantly increased as the culture time increased.

It could be inferred that, in terms of cell proliferation, 3D keratin ultrafine fibrous scaffolds were advantageous over the 2D PLA fibrous scaffolds, 3D commercial nonfibrous PCPU scaffolds, and 3D soy protein ultrafine fibrous scaffolds, which had similar morphological characteristics. Three factors might be attributed to the remarkably better cell culture results on 3D keratin scaffolds than 2D PLA, 3D commercial, and 3D soy protein scaffolds. First, keratin had cell binding motifs, like RGD and LDV in the molecules,[16] while PLA, PCPU, and soy protein did not. Second, keratin scaffolds could maintain their fibrous structures after incubation in aqueous environments in the 15 days as demonstrated in Figure 4. Third, the fibrous structures of the scaffolds could provide better guidance and support for stem cell growth, communication, and differentiation.

Chondrogenic Differentiation of ADMSCs. Figure 7 demonstrates that total collagen and GAG contents were much higher and increased much faster on 3D electrospun keratin

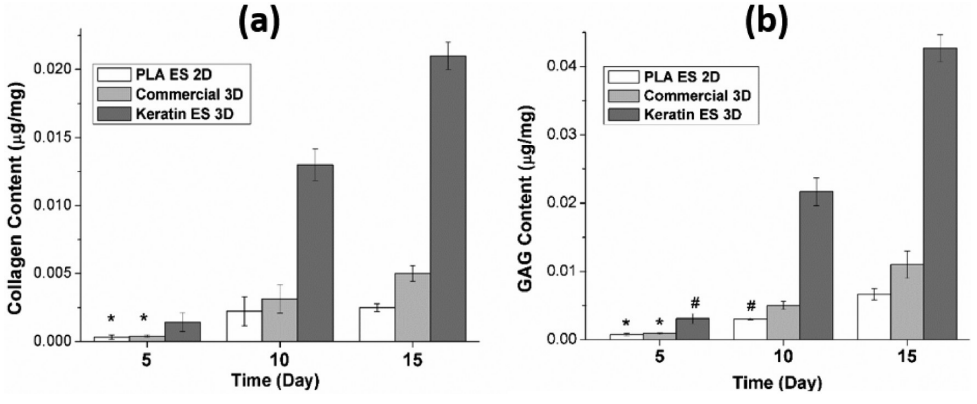

Figure 7. Quantification of (a) total collagen and (b) GAG after the initiation of chondrogenic differentiation of ADMSCs on 2D electrospun PLA scaffolds, 3D commercial scaffolds, and electrospun 3D fibrous keratin scaffolds. Data labeled with the same symbols were not significantly different from each other.

dx.doi.org/10.1021/la500768b | Langmuir 2014, 30, 8461−8470

scaffolds than on 2D PLA scaffolds and 3D commercial scaffolds after the initiation of the chondrogenic differentiation of ADMSCs. It could be seen that after 5 days of differentiation the total collagen and GAGs on the 3D keratin scaffolds were remarkably increased compared to the other two controls. On the 5th, 10th, and 15th days of chondrogenic differentiation, the weight of GAG on 3D keratin scaffolds was 4.0, 7.1, and 6.5 times that on 2D PLA and 3.4, 4.3, and 3.9 times that on 3D commercial scaffolds. And the weight of collagen on 3D keratin scaffolds was 4.3, 5.8, and 7.5 times that on 2D PLA and 3.6, 4.1, and 4.2 times that on 3D commercial scaffolds. A better guidance of fibers and preferred compositions could be attributed to the enhanced chondrogenic differentiation of ADMSCs on the 3D keratin scaffolds.

Compression Properties. Figure 8 shows the unconfined compression property of electrospun ultrafine fibrous 3D scaffolds under dry and wet conditions for different time periods. The compression modulus of 3D keratin scaffolds was around 2 kPa in the dry state and decreased to around 0.8 kPa after being soaked in PBS for 12 h. The compression modulus was further stabilized at about 0.5 kPa after being in PBS for 3 and 6 days. The properties were comparable to that of other 3D porous scaffolds for cartilage tissue engineering from natural polymers, such as silk fibroin,[42,43] gelatin,[44] and chitosan.[45] However, these scaffolds from fibroin, gelatin, and chitosan had smaller pores (less than 100 μm) encompassed in sheetlike structures and thus are much tighter than the 3D fibrous structures developed in this study. Therefore, in terms of the materials themselves, the extracted keratin might be relatively stronger than other natural polymers. However, the mechanical strength of the keratin scaffolds still needs to be improved in a future study.

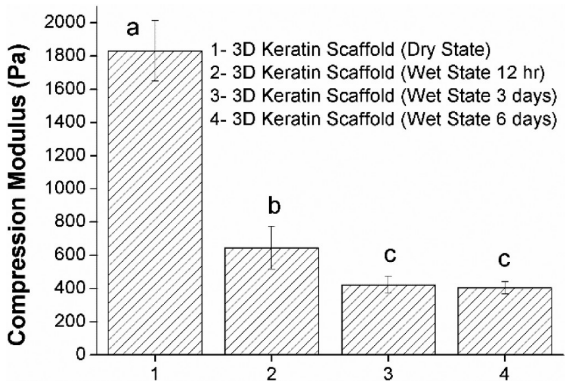

Figure 8. Compression modulus of electrospun 3D keratin fibrous scaffolds in the dry and wet states. Data labeled with the same symbols were not significantly different from each other.

CONCLUSIONS

Three-dimensional ultrafine fibrous structures from feather keratin were generated via electrospinning for cartilage tissue engineering. The keratin preserved major backbones after extraction under mild alkaline and reductive conditions. Keratin was dissolved in a nontoxic aqueous solution with an anionic surfactant, SDS. The electrospun keratin scaffolds had ultrafine fibers oriented randomly and evenly in three dimensions. The SDS could be removed from the scaffolds without affecting the 3D fibrous structures. The pure keratin fibrous scaffolds showed appreciable water stability without any chemical or physical cross-linking treatments. An in vitro study indicated that 3D keratin fibrous scaffolds could significantly better support the growth, development, and chondrogenic differentiation of adipose-derived mesenchymal stem cells than 2D PLA fibrous scaffolds, 3D commercial nonfibrous scaffolds, and 3D ultrafine fibrous scaffolds from pure soy protein. The compression modulus of the scaffolds was similar to that of many 3D scaffolds from natural polymers, though an improvement could be considered in future work. It can be concluded that the 3D ultrafine fibrous keratin structures are promising scaffold candidates for cartilage tissue engineering.

AUTHOR INFORMATION

Corresponding Author

*Tel: +001 402 472 5197. Fax: +001 402 472 0640. E-mail: yyang2@unl.edu.

Notes

The authors declare no competing financial interest.

ACKNOWLEDGMENTS

This research was financially supported by the Agricultural Research Division at the University of Nebraska—Lincoln, the USDA Hatch Act, Multistate Research Project S-1054 (NEB 37-037), and the key scientific and technological projects of the Science and Technology Commission of Shanghai Municipality no. 12JC1400300. We are grateful for the awarding of the John and Louise Skala Fellowship and an AATCC student research grant for H.X. and S.C. We also thank Dr. Han Chen for his help with SEM, Terri Fangman and Christian Elowsky for their help with CLSM, and Dr. Shadi Othman and Dr. Karin Wartella for their help with cell culturing.

REFERENCES

(1) Kim, B. S.; Mooney, D. J. Development of biocompatible synthetic extracellular matrices for tissue engineering. *Trends Biotechnol.* **1998**, *16*, 224−230.

(2) Huang, Z. H.; He, C. L.; Yang, A.; Zhang, Y.; Han, X. J.; Yin, J.; Wu, Q. Encapsulating drugs in biodegradable ultrafine fibers through co-axial electrospinning. *J. Biomed. Mater. Res., Part A* **2006**, *77*, 169−179.

(3) Son, W. K.; Youk, J. H.; Lee, T. S.; Park, W. H. The effects of solution properties and polyelectrolyte on electrospinning of ultrafine poly (ethylene oxide) fibers. *Polymer* **2004**, *45*, 2959−2966.

(4) Holzwarth, J. M.; Ma, P. X. 3D nanofibrous scaffolds for tissue engineering. *J. Mater. Chem.* **2011**, *21*, 10243−10251.

(5) Liu, X.; Ma, P. X. Phase separation, pore structure, and properties of nanofibrous gelatin scaffolds. *Biomaterials* **2009**, *30*, 4094−4103.

(6) Jiang, Q.; Reddy, N.; Zhang, S.; Roscioli, N.; Yang, Y. Water-stable electrospun collagen fibers from a non-toxic solvent and crosslinking system. *J. Biomed. Mater. Res., Part A* **2013**, *101A*, 1237−1247.

(7) Min, B. M.; Lee, G.; Kim, S. H.; Nam, Y. S.; Lee, T. S.; Park, W. H. Electrospinning of silk fibroin nanofibers and its effect on the adhesion and spreading of normal human keratinocytes and fibroblasts in vitro. *Biomaterials* **2004**, *25*, 1289−1297.

(8) Zhou, S.; Peng, H.; Yu, X.; Zheng, X.; Cui, W.; Zhang, Z.; Li, X.; Wang, J.; Weng, J.; Jia, W.; Li, F. Preparation and Characterization of a Novel Electrospun Spider Silk Fibroin/Poly(d,l-lactide) Composite Fiber. *J. Phys. Chem. B* **2008**, *112*, 11209−11216.

(9) Jiang, Q.; Reddy, N.; Yang, Y. Cytocompatible cross-linking of electrospun zein fibers for the development of water-stable tissue engineering scaffolds. *Acta Biomater.* **2010**, *6*, 4042−4051.

(10) Jiang, Q.; Yang, Y. Water-stable electrospun zein fibers for potential drug delivery. *J. Biomater. Sci., Polym. Ed.* **2011**, *22*, 1393−1408.

(11) Moroni, L.; Schotel, R.; Hamann, D.; de Wijn, J. R.; van Blitterswijk, C. A. 3D Fiber-Deposited Electrospun Integrated Scaffolds Enhance Cartilage Tissue Formation. *Adv. Funct. Mater.* **2008**, *18*, 53.
(12) Simonet, M.; Schneider, O. D.; Neuenschwander, P.; Stark, W. J. Ultraporous 3D polymer meshes by low-temperature electrospinning: use of ice crystals as a removable void template. *Polym. Eng. Sci.* **2007**, *47*, 2020−2026.
(13) Yokoyama, Y.; Hattori, S.; Yoshikawa, C.; Yasuda, Y.; Koyama, H.; Takato, T.; Kobayashi, H. Novel wet electrospinning system for fabrication of spongiform nanofiber 3-dimensional fabric. *Mater. Lett.* **2009**, *63*, 754−756.
(14) Burnett, L. R.; Rahmany, M. B.; Richter, J. R.; Aboushwareb, T. A.; Eberli, D.; Ward, C. L.; Orlando, G.; Hantgan, R. R.; Van Dyke, M. E. Hemostatic properties and the role of cell receptor recognition in human hair keratin protein hydrogels. *Biomaterials* **2013**, *34*, 2632−2640.
(15) Reichl, S.; Borrelli, M.; Geerling, G. Keratin films for ocular surface reconstruction. *Biomaterials* **2011**, *32*, 3375−3386.
(16) Tachibana, A.; Furuta, Y.; Takeshima, H.; Tanabe, T.; Yamauchi, K. Fabrication of wool keratin sponge scaffolds for long-term cell cultivation. *J. Biotechnol.* **2002**, *93*, 165−170.
(17) Tachibana, A.; Kaneko, S.; Tanabe, T.; Yamauchi, K. Rapid fabrication of keratin−hydroxyapatite hybrid sponges toward osteoblast cultivation and differentiation. *Biomaterials* **2005**, *26*, 297−302.
(18) Tanabe, T.; Okitsu, N.; Tachibana, A.; Yamauchi, K. Preparation and characterization of keratin−chitosan composite film. *Biomaterials* **2002**, *23*, 817−825.
(19) Ki, C. S.; Gang, E. H.; Um, I. C.; Park, Y. H. Nanofibrous membrane of wool keratose/silk fibroin blend for heavy metal ion adsorption. *J. Membr. Sci.* **2007**, *302*, 20−26.
(20) Li, J.; Li, Y.; Li, L.; Mak, A. F. T.; Ko, F.; Qin, L. Preparation and biodegradation of electrospun PLLA/keratin nonwoven fibrous membrane. *Polym. Degrad. Stab.* **2009**, *94*, 1800−1807.
(21) Aluigi, A.; Vineis, C.; Varesano, A.; Mazzuchetti, G.; Ferrero, F.; Tonin, C. Structure and properties of keratin/PEO blend nanofibres. *Eur. Polym. J.* **2008**, *44*, 2465−2475.
(22) Geng, X.; Kwon, O. H.; Jang, J. Electrospinning of chitosan dissolved in concentrated acetic acid solution. *Biomaterials* **2005**, *26*, 5427−5432.
(23) Jones, M. N. The interaction of sodium dodecyl sulfate with polyethylene oxide. *J. Colloid Interface Sci.* **1967**, *23*, 36−42.
(24) Moren, A. K.; Khan, A. Phase equilibria of an anionic surfactant (sodium dodecyl sulfate) and an oppositely charged protein (lysozyme) in water. *Langmuir* **1995**, *11*, 3636−3643.
(25) Ghosh, S.; Banerjee, A. A multitechnique approach in protein/surfactant interaction study: physicochemical aspects of sodium dodecyl sulfate in the presence of trypsin in aqueous medium. *Biomacromolecules* **2002**, *3*, 9−16.
(26) Cai, S.; Xu, H.; Jiang, Q.; Yang, Y. Novel 3D Electrospun Scaffolds with Fibers Oriented Randomly and Evenly in Three Dimensions to Closely Mimic the Unique Architectures of Extracellular Matrices in Soft Tissues: Fabrication and Mechanism Study. *Langmuir* **2013**, *29*, 2311−2318.
(27) Xu, H.; Jiang, Q.; Reddy, N.; Yang, Y. Hollow nanoparticles from zein for potential medical applications. *J. Mater. Chem.* **2011**, *21*, 18227−18235.
(28) Xu, H.; Zhang, Y.; Jiang, Q.; Reddy, N.; Yang, Y. Biodegradable hollow zein nanoparticles for removal of reactive dyes from wastewater. *J. Environ. Manage.* **2013**, *125*, 33−40.
(29) Li, W. J.; Tuli, R.; Okafor, C.; Derfoul, A.; Danielson, K. G.; Hall, D. J.; Tuan, R. S. A three-dimensional nanofibrous scaffold for cartilage tissue engineering using human mesenchymal stem cells. *Biomaterials* **2005**, *26*, 599−609.
(30) Erickson, G. R.; Gimble, J. M.; Franklin, D. M.; Rice, H. E.; Awad, H.; Guilak, F. Chondrogenic Potential of Adipose Tissue-Derived Stromal Cells *in Vitro* and *in Vivo*. *Biochem. Biophys. Res. Commun.* **2002**, *290*, 763−769.
(31) Levenberg, S.; Huang, N. F.; Lavik, E.; Rogers, A. B.; Itskovitz-Eldor, J.; Langer, R. Differentiation of human embryonic stem cells on three-dimensional polymer scaffolds. *Proc. Natl. Acad. Sci. U.S.A.* **2003**, *100*, 12741−12746.
(32) Wada, M.; Takagi, H. Metabolic pathways and biotechnological production of L-cysteine. *Appl. Microbiol. Biotechnol.* **2006**, *73*, 48−54.
(33) Gallezot, P. Process options for converting renewable feedstocks to bioproducts. *Green Chem.* **2007**, *9*, 295−302.
(34) Xu, H.; Yang, Y. Controlled De-Cross-Linking and Disentanglement of Feather Keratin for Fiber Preparation via a Novel Process. *ACS Sustainable Chem. Eng.* **2014**, *2*, 1404−1410.
(35) Yuan, J.; Shen, J.; Kang, I. K. Fabrication of protein-doped PLA composite nanofibrous scaffolds for tissue engineering. *Polym. Int.* **2008**, *57*, 1188−1193.
(36) Xu, H.; Cai, S.; Sellers, A.; Yang, Y. Intrinsically water-stable electrospun three-dimensional ultrafine fibrous soy protein scaffolds for soft tissue engineering using adipose derived mesenchymal stem cells. *RSC Adv.* **2014**, *4*, 15451−15457.
(37) Xu, H.; Cai, S.; Sellers, A.; Yang, Y. Electrospun ultrafine fibrous wheat glutenin scaffolds with three-dimensionally random organization and water stability for soft tissue engineering. *J. Biotechnol.* **2014**, *184*, 179−186.
(38) Suzuki, H.; Tomohiko, T. Removal of dodecyl sulfate from protein solution. *Anal. Biochem.* **1988**, *172*, 259−263.
(39) Poole, A. J.; Church, J. S.; Huson, M. G. Environmentally Sustainable Fibers from Regenerated Protein. *Biomacromolecules* **2008**, *10*, 1−8.
(40) Hu, X.; Kaplan, D.; Cebe, P. Determining beta-sheet crystallinity in fibrous proteins by thermal analysis and infrared spectroscopy. *Macromolecules* **2006**, *39*, 6161−6170.
(41) Meng, L.; Arnoult, O.; Smith, M.; Wnek, G. E. Electrospinning of in situ crosslinked collagen nanofibers. *J. Mater. Chem.* **2012**, *22*, 19412−19417.
(42) Talukdar, S.; Nguyen, Q. T.; Chen, A. C.; Sah, R. L.; Kundu, S. C. Effect of initial cell seeding density on 3D-engineered silk fibroin scaffolds for articular cartilage tissue engineering. *Biomaterials* **2011**, *32*, 8927−8937.
(43) Bhardwaj, N.; Nguyen, Q. T.; Chen, A. C.; Kaplan, D. L.; Sah, R. L.; Kundu, S. C. Potential of 3-D tissue constructs engineered from bovine chondrocytes/silk fibroin-chitosan for in vitro cartilage tissue engineering. *Biomaterials* **2011**, *32*, 5773−5781.
(44) Solorio, L. D.; Vieregge, E. L.; Dhami, C. D.; Dang, P. N.; Alsberg, E. Engineered cartilage via self-assembled hMSC sheets with incorporated biodegradable gelatin microspheres releasing transforming growth factor-β1. *J. Controlled Release* **2012**, *158*, 224−232.
(45) Neves, S. C.; Moreira Teixeira, L. S.; Moroni, L.; Reis, R. L.; Van Blitterswijk, C. A.; Alves, N. M.; Karperien, M.; Mano, J. F. Chitosan/Poly(ε-caprolactone) blend scaffolds for cartilage repair. *Biomaterials* **2011**, *32*, 1068−1079.